
Interner Bericht

**Surface Analysis using Arithmetic Operations
on Bézier Surfaces**

Thomas Schreiber

233/93

Fachbereich Informatik

Universität Kaiserslautern · Postfach 3049 · D-6750 Kaiserslautern

Interner Bericht

Surface Analysis using Arithmetic Operations on Bézier Surfaces

Thomas Schreiber

233/93

Universität Kaiserslautern
Fachbereich Informatik
Postfach 3049
D-67653 Kaiserslautern

September 1993

AG Graphische Datenverarbeitung und Computergeometrie
Prof. Dr. H. Hagen

Surface Analysis using Arithmetic Operations on Bézier Surfaces

Thomas Schreiber
University of Kaiserslautern
FB Informatik
Postfach 3049
D-67653 Kaiserslautern / Germany
e-mail: schreib@informatik.uni-kl.de

Abstract

This paper describes some new algorithms for the accurate calculation of surface properties. In the first part an arithmetic on Bézier surfaces is introduced. Formulas are given, which determine the Bézier points and weights of the resulting surface from the points and weights of the operand surfaces. An application of the arithmetic operations to the surface interrogation methods are described in the second part. It turns out, that the quality analysis can be reduced to a few numerical stable operations. Finally the advantages and disadvantages of this method are discussed.

Keywords: Arithmetic operations, Bézier surfaces, surface interrogation

1. Introduction

With increasing popularity of freeform surfaces in the area of computer aided geometric design and manufacturing the need for efficient and powerful surface interrogation tools increases. In the past many algorithms have been developed (for surveys see [11,12]). These analysis methods were derived either from the surface properties themselves [2,8,21] or from the applied geometric optics [4,13,14,17,18,22]. While a wide range of methods are currently available the more formidable problem of accurate computation has received little attention.

So far all calculation algorithms work pointwise on a predefined grid, in most cases with the possibility of an adaptive refinement. Usually an approximation surface is fitted through the grid points afterwards. If the grid is not dense enough or the approximation is not carefully done errors can arise, especially for highly sensitive data like curvature. However, there is no guarantee to find all irregularities with this technique.

Farouki and Rajan [10] showed that the results of operations like addition and multiplication with Bézier curves could be written in Bézier form too. Here we extend these operations to rational, and non rational tensor product, and triangular Bézier surfaces (see Section 3). As necessary for many applications, the extension to rational surfaces allows a division of two surfaces. In Section 4 we apply some surface interrogation methods and obtain exact representations of the property surfaces, for instance the surface of the Gaussian curvature. Because the surface degree will rise very quick, we chose the Bernstein-Bézier basis which guarantees the numerical stability of our algorithms [9,10] and which has nice properties too. The convex hull property allow safe result estimations and the formulation of necessary conditions for the Bézier points, e.g. a surface is convex, if there is no change in sign of the Bézier points that forms the Gaussian curvature surface. These properties met the requirements for adaptive procedures and allow the answers of such questions as:

- Is the surface convex or not?
- Which is the intervall for possible Gaussian curvature values?
- Is the surface developable?
- Does the surface contain umbilical points or flat points?
- Does the silhouette line cross the surface?
- Does a reflection line or isophote cross the surface?
- ...

2. Definition

Vectors are written in **bold**, e.g. $\mathbf{a} = (a_1, a_2, a_3)^T$ and surfaces with CAPITAL letters (often with degree informations), e.g. $\mathbf{X}^{mn}(u, v)$ is a parametric tensor product surface with degree (m, n) in (u, v) -direction respectively; $\mathbf{X}^m(\mathbf{u})$ is a surface of degree m over a triangular domain. The scalar and vector product of two vectors \mathbf{a} and \mathbf{b} are denoted as $\langle \mathbf{a}, \mathbf{b} \rangle$ or $\mathbf{a} \times \mathbf{b}$ respectively.

A *tensor product Bézier surface* (short: TPB) $\mathbf{X}^{mn}(u, v)$ is defined by

$$\mathbf{X}^{mn}(u, v) = \sum_{i=0}^m \sum_{j=0}^n \mathbf{b}_{ij} B_i^m(u) B_j^n(v) \quad (2.1)$$

and a *rational tensor product Bézier surface* (short: RTPB) $\mathbf{X}^{mn}(u, v)$ by

$$\mathbf{X}^{mn}(u, v) = \frac{\sum_{i=0}^m \sum_{j=0}^n \beta_{ij} \mathbf{b}_{ij} B_i^m(u) B_j^n(v)}{\sum_{i=0}^m \sum_{j=0}^n \beta_{ij} B_i^m(u) B_j^n(v)}. \quad (2.2)$$

The points \mathbf{b}_{ij} are called *Bézier points* and the β_{ij} are their *weights*. The Bézier points form the *Bézier net*, in which convex hull the entire surface lies (assuming positive weights). The basis is formed by the *Bernstein polynomials*:

$$B_i^n(t) = \binom{n}{i} t^i (1-t)^{n-i} \quad \text{with } i = 0, 1, \dots, n. \quad (2.3)$$

A Bézier surface over a triangular domain, in the following called *Bézier triangle* (short: BTR), $\mathbf{X}^m(\mathbf{u})$ of degree m is given by

$$\mathbf{X}^m(\mathbf{u}) = \sum_{|\mathbf{i}|=m} \mathbf{b}_{\mathbf{i}} B_{\mathbf{i}}^m(\mathbf{u}) \quad (2.4)$$

and a *rational Bézier triangle* (short: RBTR) $\mathbf{X}^m(\mathbf{u})$ by

$$\mathbf{X}^m(\mathbf{u}) = \frac{\sum_{|\mathbf{i}|=m} \beta_{\mathbf{i}} \mathbf{b}_{\mathbf{i}} B_{\mathbf{i}}^m(\mathbf{u})}{\sum_{|\mathbf{i}|=m} \beta_{\mathbf{i}} B_{\mathbf{i}}^m(\mathbf{u})} \quad (2.5)$$

with the *barycentric coordinates* $\mathbf{u} = (u, v, w)^T$, ($u + v + w = 1$) and indices $\mathbf{i} = (i, j, k)^T$ with $|\mathbf{i}| = m$ as $i + j + k = m$ and $i, j, k \geq 0$. The points $\mathbf{b}_{\mathbf{i}}$ are again called *Bézier points* and the $\beta_{\mathbf{i}}$ *weights*. The basis is formed by the *generalized Bernstein polynomials*:

$$B_{\mathbf{i}}^m(\mathbf{u}) = \binom{m}{\mathbf{i}} u^i v^j w^k = \frac{m!}{i!j!k!} u^i v^j w^k \quad \text{with } |\mathbf{i}| = m. \quad (2.6)$$

The formulas as well as the computations become much easier, if *scaled Bézier points* are used. They are obtained by the multiplication of the Bézier points and the corresponding binomial coefficients of the Bernstein polynomials [10]. In the triangular case this form is also called *modified Bernstein-Bézier* representation [24]. The scaled Bézier points are determined by

$$\tilde{\mathbf{b}}_{ij} = \binom{m}{i} \binom{n}{j} \mathbf{b}_{ij} \quad \text{resp.} \quad \tilde{\mathbf{b}}_{\mathbf{i}} = \binom{m}{\mathbf{i}} \mathbf{b}_{\mathbf{i}}. \quad (2.7)$$

For rational surfaces only the binomial coefficients are multiplied with the weights:

$$\tilde{\mathbf{b}}_{ij} = \mathbf{b}_{ij}, \quad \tilde{\beta}_{ij} = \binom{m}{i} \binom{n}{j} \beta_{ij} \quad \text{resp.} \quad \tilde{\mathbf{b}}_{\mathbf{i}} = \mathbf{b}_{\mathbf{i}}, \quad \tilde{\beta}_{\mathbf{i}} = \binom{m}{\mathbf{i}} \beta_{\mathbf{i}}. \quad (2.8)$$

It is advisable not to make evaluations, e.g. with the Casteljau algorithm in the scaled basis, because the convex hull property is not valid and thus the algorithms lack stability.

For more informations on Bézier surfaces see [3,5,7,15].

3. Arithmetic Operations on Bézier Surfaces

In this Section we describe an arithmetic on Bézier surfaces [25]. We give formulas, which determine the Bézier points and weights of the resulting surface from the Bézier points and weights of the operand surfaces. Concerning the scaled representations, we assume to have two functions which scale the Bézier points before starting with arithmetic operations and rescale back into the Bernstein-Bézier form afterwards.

It is fundamental that the multiplication of two Bernstein polynomials may be written as a Bernstein polynomial

$$B_i^m(t)B_j^n(t) = \frac{\binom{m}{i}\binom{n}{j}}{\binom{m+n}{i+j}}B_{i+j}^{m+n}(t). \quad (3.1)$$

To see this, we use the definition (2.3) of the Bernstein polynomials:

$$\begin{aligned} B_i^m(t)B_j^n(t) &= \binom{m}{i}t^i(1-t)^{m-i}\binom{n}{j}t^j(1-t)^{n-j} = \binom{m}{i}\binom{n}{j}t^{i+j}(1-t)^{m+n-i-j} \\ &= \frac{\binom{m}{i}\binom{n}{j}}{\binom{m+n}{i+j}}\binom{m+n}{i+j}t^{i+j}(1-t)^{m+n-(i+j)} = \frac{\binom{m}{i}\binom{n}{j}}{\binom{m+n}{i+j}}B_{i+j}^{m+n}(t). \end{aligned}$$

We immediatly get for the Bernstein polynomials of TPB and BTR:

$$B_i^m(u)B_j^n(v)B_k^p(u)B_l^q(v) = \frac{\binom{m}{i}\binom{n}{j}\binom{p}{k}\binom{q}{l}}{\binom{m+p}{i+k}\binom{n+q}{j+l}}B_{i+k}^{m+p}(u)B_{j+l}^{n+q}(v) \quad (3.2)$$

$$B_i^m(u)B_j^n(u) = \frac{\binom{m}{i}\binom{n}{j}}{\binom{m+n}{i+j}}B_{i+j}^{m+n}(u). \quad (3.3)$$

If all weights are equal, we obtain the non rational Bézier surfaces. It would be sufficient to give formulas only for the more general rational case. However for many operations (consider derivatives) the degree will rise unnecessary. Thus we will split the rational surfaces into two non rationals and apply the arithmetic on these surfaces. Before proceeding with this discussion we consider first the elementary operations on non rational Bézier surfaces.

3.1 Operations on non Rational Bézier Surfaces

3.1.1 Products

The result of the multiplication of two Bézier surfaces may be written as a Bézier surface. Let $A^{m_1, n_1}(u, v)$ be a functional Bézier surface and $B^{m_2, n_2}(u, v)$ a vector valued surface in Bézier form. Then the scaled Bézier points \tilde{c}_{pq} of the resulting surface $C^{m_1+m_2, n_1+n_2}(u, v) = A^{m_1, n_1}(u, v)B^{m_2, n_2}(u, v)$, are determined by (the denomination of the Bézier points corresponds to the surfaces of which they come from):

$$\tilde{c}_{pq} = \sum_{\substack{i+k=p \\ j+l=q}} \tilde{a}_{ij}\tilde{b}_{kl} \quad (3.4)$$

with $0 \leq i \leq m_1$, $0 \leq j \leq n_1$, $0 \leq k \leq m_2$, $0 \leq l \leq n_2$, $p = 0, 1, \dots, m_1 + m_2$ and $q = 0, 1, \dots, n_1 + n_2$.

We will give a short proof, because this is a basic formula and others are obtained in a similar way.

By the definition (2.1) we get:

$$A^{m_1, n_1}(u, v)B^{m_2, n_2}(u, v) = \sum_{i=0}^{m_1} \sum_{j=0}^{n_1} a_{ij} B_i^{m_1}(u) B_j^{n_1}(v) \sum_{k=0}^{m_2} \sum_{l=0}^{n_2} b_{kl} B_k^{m_2}(u) B_l^{n_2}(v)$$

with (3.2) and moving factors into the inner sums we obtain:

$$= \sum_{i=0}^{m_1} \sum_{j=0}^{n_1} \sum_{k=0}^{m_2} \sum_{l=0}^{n_2} a_{ij} b_{kl} \frac{\binom{m_1}{i} \binom{n_1}{j} \binom{m_2}{k} \binom{n_2}{l}}{\binom{m_1+m_2}{i+k} \binom{n_1+n_2}{j+l}} B_{i+k}^{m_1+m_2}(u) B_{j+l}^{n_1+n_2}(v)$$

with scaled Bézier points (2.7) and rearranging the sums (with $p = i + k$, $q = j + l$) we finally get:

$$\begin{aligned} &= \sum_{p=0}^{m_1+m_2} \sum_{q=0}^{n_1+n_2} \frac{1}{\binom{m_1+m_2}{p} \binom{n_1+n_2}{q}} \sum_{\substack{i+k=p \\ j+l=q}} \tilde{a}_{ij} \tilde{b}_{kl} B_p^{m_1+m_2}(u) B_q^{n_1+n_2}(v) \\ &= \sum_{p=0}^{m_1+m_2} \sum_{q=0}^{n_1+n_2} c_{pq} B_p^{m_1+m_2}(u) B_q^{n_1+n_2}(v) = C^{m_1+m_2, n_1+n_2}(u, v). \end{aligned}$$

Writing c_{pq} in the scaled form completes the proof. \square

For the multiplication of two BTR $C^{m+n}(u) = A^m(u)B^n(u)$ the scaled Bézier points of the resulting surface are determined by:

$$\tilde{c}_k = \sum_{|i|+|j|=|k|} \tilde{a}_i \tilde{b}_j \quad (3.5)$$

with $|i| = m$, $|j| = n$ and $|k| = m + n$.

Remark:

The degree elevation of a Bézier surface turns out to be a special multiplication with a surface of which all Bézier points are equal to 1. Let \tilde{b}_{pq} the Bézier points of the TPB $X^{m+r, n+s}(u, v)$ which were obtained by a degree elevation of $X^{mn}(u, v)$ with Bézier points a_{ij} . Thus we have

$$\tilde{b}_{pq} = \sum_{\substack{i+k=p \\ j+l=q}} \tilde{a}_{ij} \binom{r}{k} \binom{s}{l} \quad (3.6)$$

with $0 \leq i \leq m$, $0 \leq j \leq n$, $0 \leq k \leq r$, $0 \leq l \leq s$, $p=0, 1, \dots, m+r$ and $q=0, 1, \dots, n+s$.

For the Bézier points \tilde{b}_k of the degree elevated BTR $X^{m+r}(u)$ we get:

$$\tilde{b}_k = \sum_{|i|+|j|=|k|} \tilde{a}_i \binom{r}{j} \quad (3.7)$$

with \mathbf{a}_i as the Bézier points of $\mathbf{X}^m(u)$, $|i| = m$, $|j| = r$ and $|k| = m + r$.

We multiply \mathbf{X} with the surface:

$$Y^{rs}(u, v) = \sum_{k=0}^r \sum_{l=0}^s B_k^r(u) B_l^s(v) \equiv 1$$

or

$$Y^r(u) = \sum_{|j|=r} B_j^r(u) \equiv 1.$$

respectively. Y is identical to 1. The multiplication changes only the degree of the surface, but not the shape. The binomial coefficients in formula (3.6) and (3.7) correspond to the scaled form of the Bézier points of Y , which are all equal to 1.

For the scalar and vector product of two TPB $\mathbf{A}^{m_1, n_1}(u, v)$ and $\mathbf{B}^{m_2, n_2}(u, v)$ we obtain for the scalar product the functional surface $C^{m_1+m_2, n_1+n_2}(u, v) = \langle \mathbf{A}^{m_1, n_1}, \mathbf{B}^{m_2, n_2} \rangle$ by

$$\tilde{c}_{pq} = \sum_{\substack{i+k=p \\ j+l=q}} \langle \tilde{\mathbf{a}}_{ij}, \tilde{\mathbf{b}}_{kl} \rangle \quad (3.8)$$

and for the vector product the Bézier points \mathbf{c}_{pq} of the vector valued TPB $C^{m_1+m_2, n_1+n_2} = \mathbf{A}^{m_1, n_1} \times \mathbf{B}^{m_2, n_2}$ by

$$\tilde{\mathbf{c}}_{pq} = \sum_{\substack{i+k=p \\ j+l=q}} \tilde{\mathbf{a}}_{ij} \times \tilde{\mathbf{b}}_{kl} \quad (3.9)$$

with $0 \leq i \leq m_1$, $0 \leq j \leq n_1$, $0 \leq k \leq m_2$, $0 \leq l \leq n_2$, $p = 0, 1, \dots, m_1 + m_2$ and $q = 0, 1, \dots, n_1 + n_2$.

The application to BTR yields

$$\tilde{c}_k = \sum_{|i|+|j|=|k|} \langle \tilde{\mathbf{a}}_i, \tilde{\mathbf{b}}_j \rangle \quad (3.10)$$

and

$$\tilde{\mathbf{c}}_k = \sum_{|i|+|j|=|k|} \tilde{\mathbf{a}}_i \times \tilde{\mathbf{b}}_j \quad (3.11)$$

with $|i| = m$, $|j| = n$ and $|k| = m + n$.

3.1.2 Addition and Subtraction

Before we can add or subtract two Bézier surfaces we have to express them in the same degree. Then the addition or subtraction becomes trivial.

For the TPB $C^{mn}(u, v) = A^{mn}(u, v) \pm B^{mn}(u, v)$ we get:

$$c_{ij} = a_{ij} \pm b_{ij} \quad (3.12)$$

with $i=0, 1, \dots, m$ and $j=0, 1, \dots, n$.

Analog we get for BTR $C^l(u) = A^l(u) \pm B^l(u)$:

$$c_i = a_i \pm b_i \quad (3.13)$$

with $|i| = l$.

After combination of degree elevation and addition or subtraction we obtain for TPB:

$$\tilde{c}_{pq} = \sum_{\substack{i+k=p \\ j+l=q}} \tilde{a}_{ij} \binom{m-m_1}{k} \binom{n-n_1}{l} \pm \tilde{b}_{kl} \binom{m-m_2}{i} \binom{n-n_2}{j} \quad (3.14)$$

with $0 \leq i \leq m_1$, $0 \leq j \leq n_1$, $0 \leq k \leq m_2$, $0 \leq l \leq n_2$, $p=0, 1, \dots, m$, $q=0, 1, \dots, n$ and with $m = \max(m_1, m_2)$ and $n = \max(n_1, n_2)$.

For the BTR $C^l(u) = A^m(u) \pm B^n(u)$ we get:

$$\tilde{c}_k = \sum_{|i|+|j|=|k|} \tilde{a}_i \binom{l-m}{j} \pm \tilde{b}_j \binom{l-n}{i} \quad (3.15)$$

with $|i| = m$, $|j| = n$, $|k| = l$ and $l = \max(m, n)$.

3.1.3 Division

For the division of two Bézier surfaces the divisor surface has to be a functional surface (one can not divide through vectors!). Unlike the division in [10] the result here is always a rational Bézier surface. Like Section 3.1.2 both surfaces must have the same degree. This may be obtained by an appropriate degree elevation with (3.6) or (3.7). Then the division also becomes trivial. For the TPB $C^{mn}(u, v) = A^{mn}(u, v)/B^{mn}(u, v)$ we get:

$$\begin{aligned} c_{ij} &= \frac{a_{ij}}{b_{ij}} \\ \gamma_{ij} &= b_{ij} \end{aligned} \quad (3.16)$$

with $i=0, 1, \dots, m$ and $j=0, 1, \dots, n$. The γ_{ij} are the weights of the RTPB $C^{mn}(u, v)$.

Analog we get the Bézier points and weights for the BTR $C^m(u) = A^m(u)/B^m(u)$ by

$$\begin{aligned} c_i &= \frac{a_i}{b_i} \\ \gamma_i &= b_i \end{aligned} \quad (3.17)$$

with $|\mathbf{i}| = m$.

The combination of degree elevation and division for the TPB $C^{m,n}(u, v) = \mathbf{A}^{m_1, n_1}(u, v) / \mathbf{B}^{m_2, n_2}(u, v)$ with $m = \max(m_1, m_2)$ und $n = \max(n_1, n_2)$ yields:

$$\begin{aligned}\tilde{c}_{pq} &= \frac{1}{\tilde{\gamma}_{pq}} \sum_{\substack{i+k=p \\ j+l=q}} \tilde{a}_{ij} \binom{m-m_1}{k} \binom{n-n_1}{l} \\ \tilde{\gamma}_{pq} &= \sum_{\substack{i+k=p \\ j+l=q}} \tilde{b}_{kl} \binom{m-m_2}{i} \binom{n-n_2}{j}\end{aligned}\tag{3.18}$$

with $0 \leq i \leq m_1$, $0 \leq j \leq n_1$, $0 \leq k \leq m_2$, $0 \leq l \leq n_2$, $p=0, 1, \dots, m$ and $q=0, 1, \dots, n$.

For the application to BTR $C^l(\mathbf{u}) = \mathbf{A}^m(\mathbf{u}) / \mathbf{B}^n(\mathbf{u})$ with $l = \max(m, n)$ we get:

$$\begin{aligned}\tilde{c}_{\mathbf{k}} &= \frac{1}{\tilde{\gamma}_{\mathbf{k}}} \sum_{|\mathbf{i}|+|\mathbf{j}|=|\mathbf{k}|} \tilde{a}_{\mathbf{i}} \binom{l-m}{\mathbf{j}} \\ \tilde{\gamma}_{\mathbf{k}} &= \sum_{|\mathbf{i}|+|\mathbf{j}|=|\mathbf{k}|} \tilde{b}_{\mathbf{j}} \binom{l-n}{\mathbf{i}}\end{aligned}\tag{3.19}$$

with $|\mathbf{i}| = m$, $|\mathbf{j}| = n$ and $|\mathbf{k}| = l$.

3.2 Operations on Rational Bézier Surfaces

The division of two Bézier surfaces generates always a rational surface. Thus the operations have to be extended to rational surfaces even if only non rational input surfaces were used.

As mentioned above any rational surface may be decomposed into two non rational surfaces: a nominator surface Z and a denominator surface N . The latter is a functional surface.

$$\mathbf{A}^{m,n}(u, v) = \frac{Z^{m,n}(u, v)}{N^{m,n}(u, v)} \quad \text{resp.} \quad \mathbf{A}^m(\mathbf{u}) = \frac{Z^m(\mathbf{u})}{N^m(\mathbf{u})}.$$

The associated Bézier points z_{ij} and n_{ij} are given by

$$\begin{aligned}z_{ij} &= \alpha_{ij} \mathbf{a}_{ij} \\ n_{ij} &= \alpha_{ij}\end{aligned} \quad \text{resp.} \quad \begin{aligned}z_{\mathbf{i}} &= \alpha_{\mathbf{i}} \mathbf{a}_{\mathbf{i}} \\ n_{\mathbf{i}} &= \alpha_{\mathbf{i}}\end{aligned}$$

where $0 \leq i \leq m$, $0 \leq j \leq n$ and $|\mathbf{i}| = m$.

With this splitting procedure the arithmetic operations on rational surfaces can be expressed by operations with non rational surfaces. This also simplifies the combination with rational and non rational surfaces. For completion we list the results in the following:

$$C^{m_1+m_2, n_1+n_2}(u, v) = A^{m_1, n_1}(u, v) B^{m_2, n_2}(u, v):$$

$$\begin{aligned}\tilde{c}_{pq} &= \frac{1}{\tilde{\gamma}_{pq}} \sum_{\substack{i+k=p \\ j+l=q}} \tilde{\alpha}_{ij} \tilde{\beta}_{kl} \tilde{a}_{ij} \tilde{b}_{kl} \\ \tilde{\gamma}_{pq} &= \sum_{\substack{i+k=p \\ j+l=q}} \tilde{\alpha}_{ij} \tilde{\beta}_{kl}\end{aligned}\tag{3.20}$$

$$C^{m_1+m_2, n_1+n_2}(u, v) = \langle A^{m_1, n_1}(u, v), B^{m_2, n_2}(u, v) \rangle:$$

$$\begin{aligned}\tilde{c}_{pq} &= \frac{1}{\tilde{\gamma}_{pq}} \sum_{\substack{i+k=p \\ j+l=q}} \tilde{\alpha}_{ij} \tilde{\beta}_{kl} \langle \tilde{a}_{ij}, \tilde{b}_{kl} \rangle \\ \tilde{\gamma}_{pq} &= \sum_{\substack{i+k=p \\ j+l=q}} \tilde{\alpha}_{ij} \tilde{\beta}_{kl}\end{aligned}\tag{3.21}$$

$$C^{m_1+m_2, n_1+n_2}(u, v) = A^{m_1, n_1}(u, v) \times B^{m_2, n_2}(u, v):$$

$$\begin{aligned}\tilde{c}_{pq} &= \frac{1}{\tilde{\gamma}_{pq}} \sum_{\substack{i+k=p \\ j+l=q}} \tilde{\alpha}_{ij} \tilde{\beta}_{kl} (\tilde{a}_{ij} \times \tilde{b}_{kl}) \\ \tilde{\gamma}_{pq} &= \sum_{\substack{i+k=p \\ j+l=q}} \tilde{\alpha}_{ij} \tilde{\beta}_{kl}\end{aligned}\tag{3.22}$$

$$C^{m_1+m_2, n_1+n_2}(u, v) = A^{m_1, n_1}(u, v) \pm B^{m_2, n_2}(u, v):$$

$$\begin{aligned}\tilde{c}_{pq} &= \frac{1}{\tilde{\gamma}_{pq}} \sum_{\substack{i+k=p \\ j+l=q}} \tilde{\alpha}_{ij} \tilde{\beta}_{kl} (\tilde{a}_{ij} \pm \tilde{b}_{kl}) \\ \tilde{\gamma}_{pq} &= \sum_{\substack{i+k=p \\ j+l=q}} \tilde{\alpha}_{ij} \tilde{\beta}_{kl}\end{aligned}\tag{3.23}$$

$$C^{m_1+m_2, n_1+n_2}(u, v) = A^{m_1, n_1}(u, v) / B^{m_2, n_2}(u, v):$$

$$\begin{aligned}\tilde{c}_{pq} &= \frac{1}{\tilde{\gamma}_{pq}} \sum_{\substack{i+k=p \\ j+l=q}} \tilde{\alpha}_{ij} \tilde{\beta}_{kl} \tilde{a}_{ij} \\ \tilde{\gamma}_{pq} &= \sum_{\substack{i+k=p \\ j+l=q}} \tilde{\alpha}_{ij} \tilde{\beta}_{kl} \tilde{b}_{kl}\end{aligned}\tag{3.24}$$

with $0 \leq i \leq m_1$, $0 \leq j \leq n_1$, $0 \leq k \leq m_2$, $0 \leq l \leq n_2$, $p = 0, 1, \dots, m_1 + m_2$ and $q = 0, 1, \dots, n_1 + n_2$.

$$C^{m+n}(u) = A^m(u)B^n(u):$$

$$\begin{aligned}\tilde{c}_k &= \frac{1}{\tilde{\gamma}_{pq}} \sum_{|i|+|j|=|k|} \tilde{\alpha}_i \tilde{\beta}_j \tilde{a}_i \tilde{b}_j \\ \tilde{\gamma}_k &= \sum_{|i|+|j|=|k|} \tilde{\alpha}_i \tilde{\beta}_j\end{aligned}\tag{3.25}$$

$$C^{m+n}(u) = \langle A^m(u), B^n(u) \rangle:$$

$$\begin{aligned}\tilde{c}_k &= \frac{1}{\tilde{\gamma}_k} \sum_{|i|+|j|=|k|} \tilde{\alpha}_i \tilde{\beta}_j \langle \tilde{a}_i, \tilde{b}_j \rangle \\ \tilde{\gamma}_k &= \sum_{|i|+|j|=|k|} \tilde{\alpha}_i \tilde{\beta}_j\end{aligned}\tag{3.26}$$

$$C^{m+n}(u) = A^m(u) \times B^n(u):$$

$$\begin{aligned}\tilde{c}_k &= \frac{1}{\tilde{\gamma}_k} \sum_{|i|+|j|=|k|} \tilde{\alpha}_i \tilde{\beta}_j (\tilde{a}_i \times \tilde{b}_j) \\ \tilde{\gamma}_k &= \sum_{|i|+|j|=|k|} \tilde{\alpha}_i \tilde{\beta}_j\end{aligned}\tag{3.27}$$

$$C^{m+n}(u) = A^m(u) \pm B^n(u):$$

$$\begin{aligned}\tilde{c}_k &= \frac{1}{\tilde{\gamma}_{pq}} \sum_{|i|+|j|=|k|} \tilde{\alpha}_i \tilde{\beta}_j (\tilde{a}_i \pm \tilde{b}_j) \\ \tilde{\gamma}_k &= \sum_{|i|+|j|=|k|} \tilde{\alpha}_i \tilde{\beta}_j\end{aligned}\tag{3.28}$$

$$C^{m+n}(u) = A^m(u)/B^n(u):$$

$$\begin{aligned}\tilde{c}_k &= \frac{1}{\tilde{\gamma}_{pq}} \sum_{|i|+|j|=|k|} \tilde{\alpha}_i \tilde{\beta}_j \tilde{a}_i \\ \tilde{\gamma}_k &= \sum_{|i|+|j|=|k|} \tilde{\alpha}_i \tilde{\beta}_j \tilde{b}_j\end{aligned}\tag{3.29}$$

with $|i| = m$, $|j| = n$ and $|k| = m + n$.

Remarks:

1. For addition, subtraction and division of rational surfaces is no degree elevation necessary. The degree rise to the sum of the degrees of both operand surfaces.
2. A constant, vector or curve may be written as a Bézier surface (with an adequate zero degree) and combined with other surfaces as described above.
3. All operations are independent of the parametrization as long as both operand surfaces have the same parametrization.
4. The commutative, associative and distributive laws are carried over from the vector arithmetic to the Bézier surface arithmetic.

3.3 Derivatives and Integration of Bézier Surfaces

The derivatives and integration of Bézier surfaces (integration only for non rational Bézier surfaces) are well known, e.g. from [3,5,7,15]. Thus they were omitted here. We will only remark, that the derivatives of rational surfaces may be computed with only one division at the end of the computation. The integration yields a vector or constant result.

3.4 Implementation

The given formulas are not suitable for implementations. The indices of the sums can be evaluated directly, e.g. for the multiplication of two TPB or BTR we get respectively:

$$\tilde{c}_{kl} = \sum_{i=\max(0, k-m_2)}^{\min(k, m_1)} \sum_{j=\max(0, l-n_2)}^{\min(l, n_1)} \tilde{a}_{ij} \tilde{b}_{k-i, l-j} \quad (3.30)$$

with $k=0, 1, \dots, m_1+m_2$ and $l=0, 1, \dots, n_1+n_2$ or

$$\tilde{c}_{m+n-k, k-l, l} = \sum_{i=\max(0, k-n)}^{\min(k, m)} \sum_{j=\max(0, l-(k-i))}^{\min(i, l)} \tilde{a}_{m-i, i-j, j} \tilde{b}_{n-(k-i), (k-i)-(l-j), l-j} \quad (3.31)$$

with $0 \leq k \leq m+n$ and $0 \leq l \leq k$.

These denominations are not used here, because of their long and unreadable indices.

4. Surface Analysis

For simplifying formulations we will give in the following only the notations of tensor product surfaces. The calculations are exactly the same for Bézier triangles.

4.1 Curvature Analysis

In the area of CAD/CAM high variations or changes in sign of the Gaussian curvature are not desirable. For visualization it is usual to evaluate the Gaussian curvature pointwise on a predefined grid and fit an approximation surface (often linear) through the grid points afterwards. If the grid is not dense enough, errors can occur, especially surface irregularities may remain hidden. The arithmetic of Section 3 enables the computation of the exact surface of the Gaussian curvature.

Let $\mathbf{X}^{mn}(u, v)$ be the investigation surface, then the *Gaussian curvature surface* $K^{pq}(u, v)$ is given by [19,20]:

$$K^{pq}(u, v) = \frac{LN - M^2}{(EG - F^2)^2} = \frac{LN - M^2}{\langle \mathbf{Y}(u, v), \mathbf{Y}(u, v) \rangle^2} \quad (4.1)$$

where

$$\begin{aligned} E &= \langle \mathbf{X}_u(u, v), \mathbf{X}_u(u, v) \rangle \\ F &= \langle \mathbf{X}_u(u, v), \mathbf{X}_v(u, v) \rangle \\ G &= \langle \mathbf{X}_v(u, v), \mathbf{X}_v(u, v) \rangle \\ L &= \langle \mathbf{X}_{uu}(u, v), \mathbf{Y}(u, v) \rangle \\ M &= \langle \mathbf{X}_{uv}(u, v), \mathbf{Y}(u, v) \rangle \\ N &= \langle \mathbf{X}_{vv}(u, v), \mathbf{Y}(u, v) \rangle \end{aligned} \quad (4.2)$$

with the partial derivatives $\mathbf{X}_u(u, v) = \frac{\partial \mathbf{X}(u, v)}{\partial u}$, $\mathbf{X}_v(u, v) = \frac{\partial \mathbf{X}(u, v)}{\partial v}$, $\mathbf{X}_{uu}(u, v) = \frac{\partial^2 \mathbf{X}(u, v)}{\partial^2 u}$, $\mathbf{X}_{uv}(u, v) = \frac{\partial^2 \mathbf{X}(u, v)}{\partial u \partial v}$ and $\mathbf{X}_{vv}(u, v) = \frac{\partial^2 \mathbf{X}(u, v)}{\partial^2 v}$.

$\mathbf{Y}(u, v)$ is called the *normal surface*:

$$\mathbf{Y}(u, v) = \mathbf{X}_u(u, v) \times \mathbf{X}_v(u, v). \quad (4.3)$$

$K^{pq}(u, v)$ is a function valued RTPB with positive weights at the vertices k_{00} , k_{p0} , k_{0q} and k_{pq} . Until interior weights are negative, a subdivision should be made to ensure that the entire surface lies in the convex hull of the Bézier points. Then the extreme values of the Gaussian curvature may be estimated by the Bézier net. If desired, further subdivisions will give better estimations. For the convexity test, it is sufficient to subdivide only the non rational nominator surface, until all Bézier points have the same sign or there exists two values with different signs at the vertices. Often only a few subdivisions are necessary to yield a definite result. Other surfaces may be tested for roots with the same procedure.

If $\mathbf{X}^{mn}(u, v)$ is non rational, $K^{pq}(u, v)$ has the degree ($p = 8m - 4$, $q = 8n - 4$) and for rational investigation surfaces the degree rises up to ($p = 16m - 4$, $q = 16n - 4$). This is

quite large, but for suitable input surfaces the locations of the Bézier points of $K^{pq}(u, v)$ are well-behaved and give a good estimation of the surface (see Figure 2).

As an example we take the well known TPB from Schelske [23]. Each parameter line of the surface is convex, but the surface is not. The Bézier points are

$$\begin{array}{cccc}
 \mathbf{b}_{00} = (0, 0, 0)^T & \mathbf{b}_{01} = (1, 0, 1)^T & \mathbf{b}_{02} = (2, 0, 2)^T & \mathbf{b}_{03} = (3, 0, 0)^T \\
 \mathbf{b}_{10} = (0, 1, 2)^T & \mathbf{b}_{11} = (1, 1, 2)^T & \mathbf{b}_{12} = (2, 1, 2)^T & \mathbf{b}_{13} = (3, 1, 1)^T \\
 \mathbf{b}_{20} = (0, 2, 1)^T & \mathbf{b}_{21} = (1, 2, 2)^T & \mathbf{b}_{22} = (2, 2, 2)^T & \mathbf{b}_{23} = (3, 2, 2)^T \\
 \mathbf{b}_{30} = (0, 3, 0)^T & \mathbf{b}_{31} = (1, 3, 2)^T & \mathbf{b}_{32} = (2, 3, 1)^T & \mathbf{b}_{33} = (3, 3, 0)^T
 \end{array}$$

Figure 1 shows the Bézier net of the example surface and Figure 2 the Bézier net of the Gaussian curvature surface. Figure 3 displays the example surface with the contour of zero Gaussian curvature and Figure 4 the surface of Gaussian curvature with the contour $K^{pq}(u, v) = 0$.

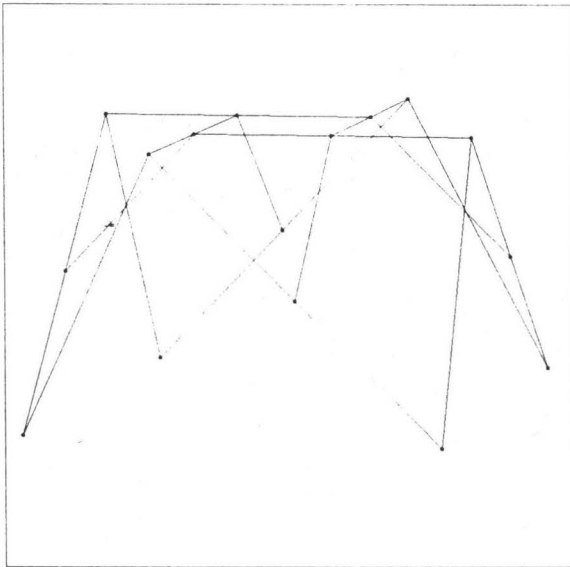


Fig. 1: Bézier net of example surface

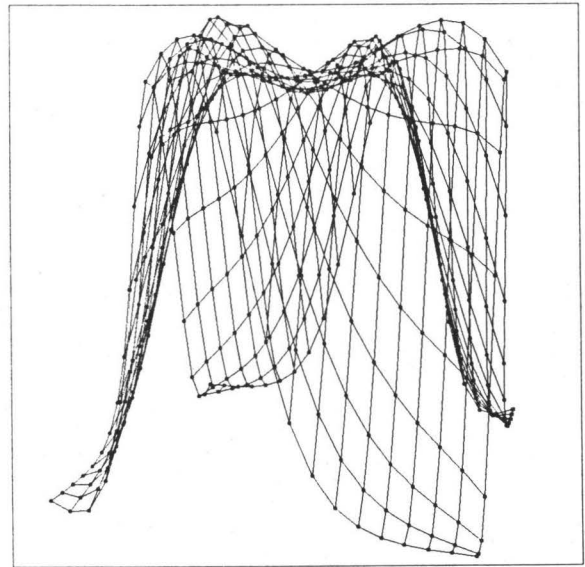


Fig. 2: Bézier net of its Gaussian curvature surface

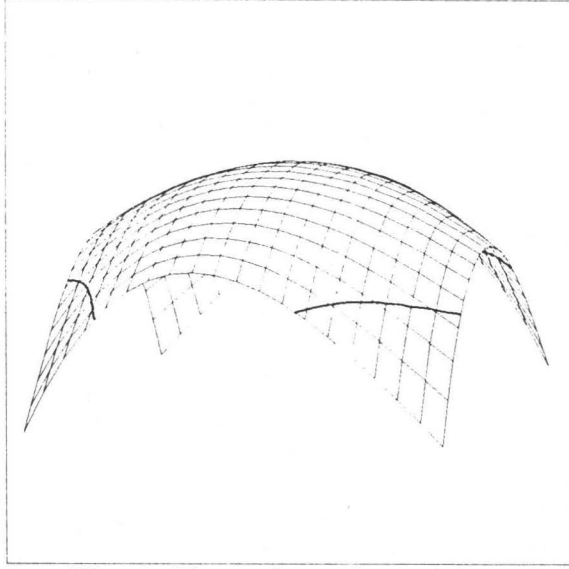


Fig. 3: Example surface with contour of $K^{pq}(u, v) = 0$

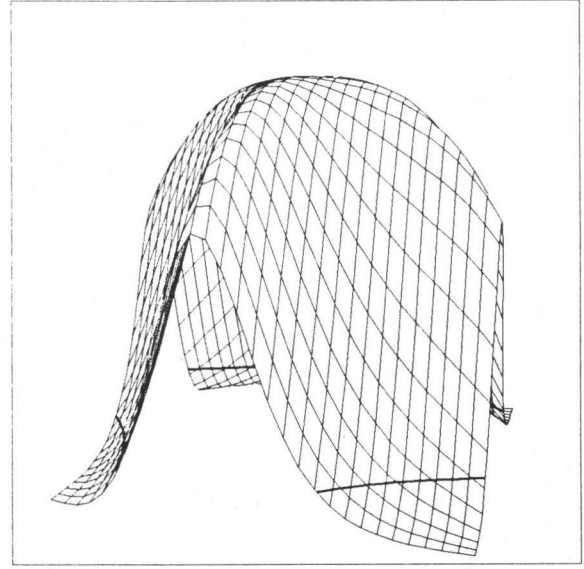


Fig. 4: Gaussian curvature surface with contour of $K^{pq}(u, v) = 0$

The intermediate surfaces (namely L , N , M and $LN - M^2$) enable a classification of the investigation surface; e.g. these surfaces allow a distinction between planes and cylinders.

The surface $\mathbf{X}^{mn}(u, v)$ is called

$$\left. \begin{array}{l} \text{elliptical} \\ \text{hyperbolic} \\ \text{flat} \\ \text{parabolic} \end{array} \right\} \text{ iff } \left. \begin{array}{l} LN - M^2 > 0 \\ LN - M^2 < 0 \\ L = N = M = 0 \iff L^2 + N^2 + M^2 = 0 \\ \text{else} \end{array} \right\} \quad (4.4)$$

is valid for the whole domain.

Also important for the surfaces analysis is the detection of umbilical points. A point on the surface at which the normal curvature is equal for all directions is called an *umbilical point*. A condition is:

$$\begin{aligned} \kappa_1 &= \kappa_2 = \text{const.} \\ \iff \kappa_1 - \kappa_2 &= 0 \\ \iff (EN + GL - 2FM)^2 - 4(LN - M^2)(EG - F^2) &= 0. \end{aligned} \quad (4.5)$$

A *flat point* is a special umbilical point which satisfy:

$$\begin{aligned} \kappa_1 &= \kappa_2 = 0 \\ \iff \kappa_1^2 + \kappa_2^2 &= 0 \\ \iff (EN + GL - 2FM)^2 - 2(LN - M^2)(EG - F^2) &= 0 \\ \iff L^2 + M^2 + N^2 &= 0 \end{aligned} \quad (4.6)$$

where κ_1 and κ_2 are the principal curvatures.

Figure 5 shows the example surface with isolines $\kappa_1 - \kappa_2 = \text{const.}$ and Figure 6 the associated *umbilical surface*. Figure 7 and 8 show the analog flat point situation.

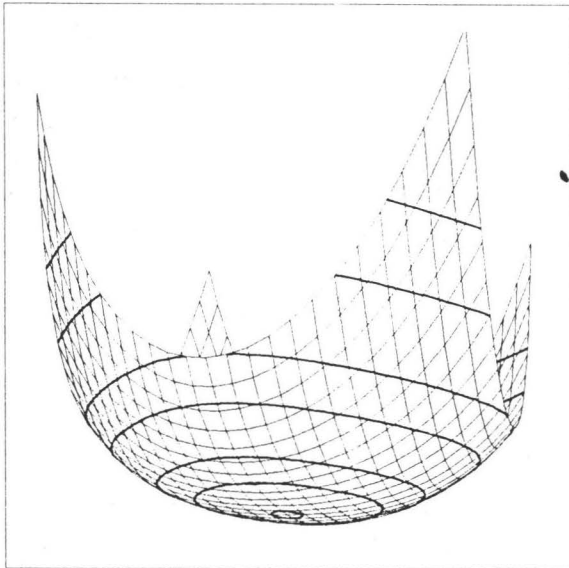


Fig. 5: Umbilical surface with contours of $\kappa_1 - \kappa_2 = \text{const.}$

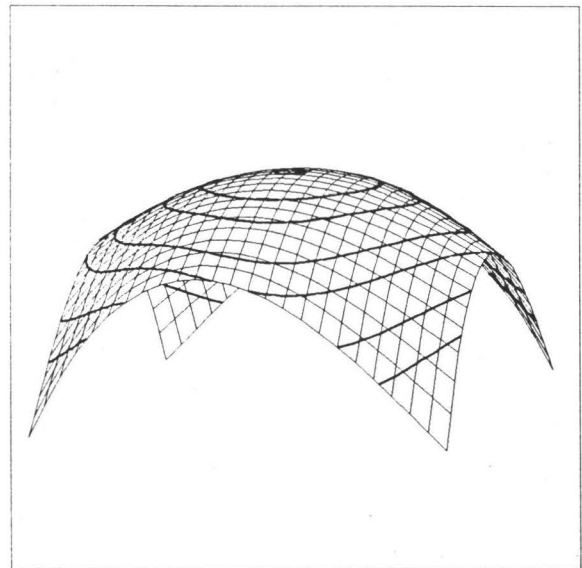


Fig. 6: Example surface with contours of $\kappa_1 - \kappa_2 = \text{const.}$

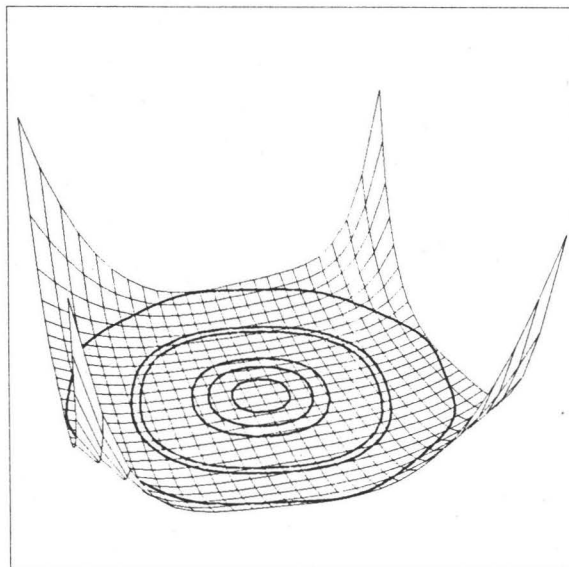


Fig. 7: Flat point surface with contours of $\kappa_1^2 + \kappa_2^2 = \text{const.}$

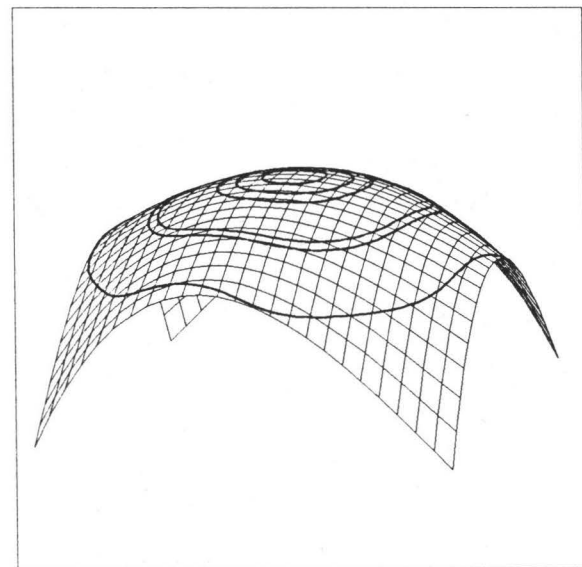


Fig. 8: Example surface with contours of $\kappa_1^2 + \kappa_2^2 = \text{const.}$

4.2 Reflection Lines

The reflection line analysis gives a quantity of the aesthetic quality of a surface [12]. Small dents were visualized by irregularities in the reflection line pattern of parallel light lines [17,18].

Often the computation of the reflection lines is difficult (solving non-linear systems of equations). With the aid of arithmetic operations the calculation degenerates to a numerical stable root finding of non rational, functional Bézier surfaces. Let $\mathbf{X}^{mn}(u, v)$ be the investigation surface, B the eye point of the observer and $\mathbf{Y}(u, v)$ the normal surface, then the *reflection surface* of all rays coming from the eye point and reflected by the surface, is determined by

$$\mathbf{S}(u, v) = 2 \frac{\mathbf{Y}(u, v) \cdot \langle \mathbf{B}(u, v), \mathbf{Y}(u, v) \rangle}{\langle \mathbf{Y}(u, v), \mathbf{Y}(u, v) \rangle} - \mathbf{B}(u, v) \quad (4.7)$$

with $\mathbf{B}(u, v) = B - \mathbf{X}(u, v)$.

The reflected rays intersect a set of light lines $g_i(t) = L_i + t\mathbf{l}$ with $i = 0, 1, \dots, n$ if and only if the *reflection surfaces* $R_i(u, v) = 0$:

$$\begin{aligned} R_i(u, v) &= \det |\mathbf{S}(u, v), \mathbf{l}, \mathbf{X}(u, v) - L_i| = 0 \\ &= \langle \mathbf{S}(u, v) \times \mathbf{l}, \mathbf{X}(u, v) - L_i \rangle = 0. \end{aligned} \quad (4.8)$$

The degree of $R_i(u, v)$ is $(7m - 2, 7n - 2)$ for non rational and $(10m - 2, 10n - 2)$ for rational investigation surfaces. For the root finding only the nominator surface is necessary.

Figure 9 shows a reflection line surface with a contour of $R(u, v) = 0$ and Figure 10 displays the interrogation surface with the reflection line.

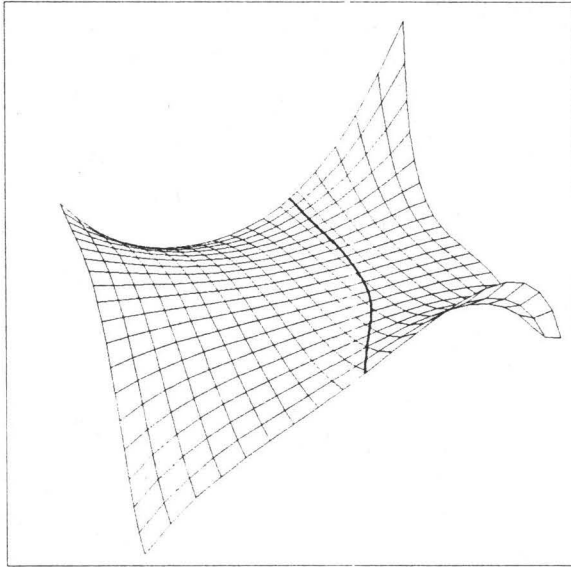


Fig. 9: Reflection line surface with contour $R(u, v) = 0$.

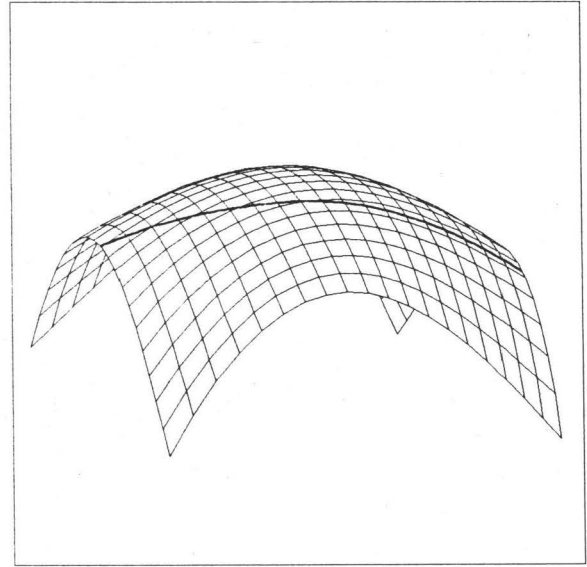


Fig. 10: Example surface with reflection line of Fig. 9.

4.3 Isophotes

Isophotes are lines of equal light intensity with respect to a given normalized light direction l . Let $Y(u, v)$ be the normal of the investigation surface $X^{mn}(u, v)$, then the isophote condition is given by [22]

$$I(u, v) = \left\langle \frac{Y(u, v)}{\|Y(u, v)\|}, l \right\rangle = c = \text{const.} \quad (4.9)$$

The silhouettes are special isophotes with $c = 0$. This is only true for parallel projections. For perspective projections we obtain the following condition for the silhouettes:

$$I(u, v) = \langle Y(u, v), A(u, v) \rangle = 0 \quad (4.10)$$

with $A(u, v) = X(u, v) - A$ and eye point A . See Figure 11 and 12 for an adaptive linear approximation with respect to the silhouette.

An easy condition is achieved for parallel projection and surfaces given in viewing coordinates. Let the z -axis be equal with the viewing direction, then it is sufficient to find only the roots for $Z(u, v) = 0$, where $Z(u, v)$ is the z -component of the normal surface.

Now let us go back to the isophotes. The normalization of (4.9) was bypassed with

$$\frac{\langle Y(u, v), l \rangle^2}{\langle Y(u, v), Y(u, v) \rangle} = c^2 \quad (4.11)$$

To take (4.11) instead of (4.9) invokes the generation of two isophotes $I(u, v) = \pm c$. This is in general no disadvantage because the user often wants to see more than just one isophote. The degree of the isophote surface is $(4m - 2, 4n - 2)$ for non rational and $(8m - 2, 8n - 2)$ for rational investigation surfaces.

If a surface is C^r -continuous, then the isophote surface consists of C^{r-1} -continuous patches and the isophotes are C^{r-1} -continuous curves. The gap in the isophote surface of Figure 13 and the gaps in the isophotes of Figure 14 prove that the patches are only C^0 -continuous; whereas the tangential discontinuity of the isophote surface in Figure 15 and of the isophotes in Figure 16 denote G^1 -continuous patches.

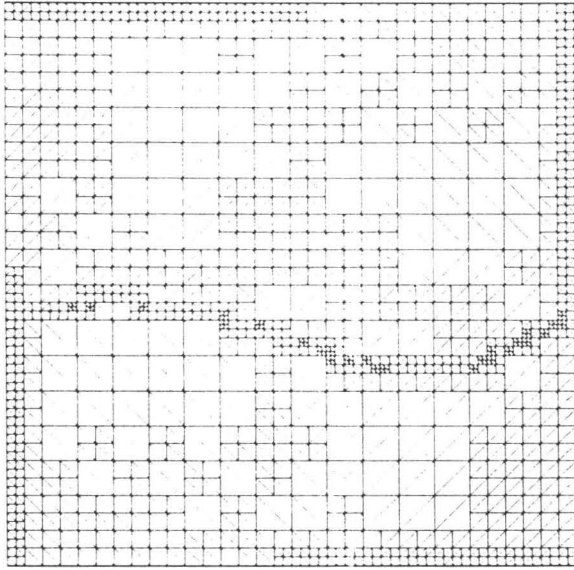


Fig. 11: Approximation in the domain

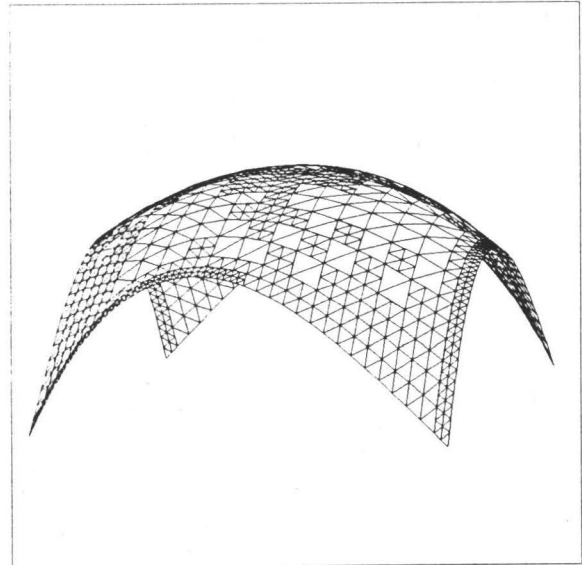


Fig. 12: Linear Approximation of the example surface

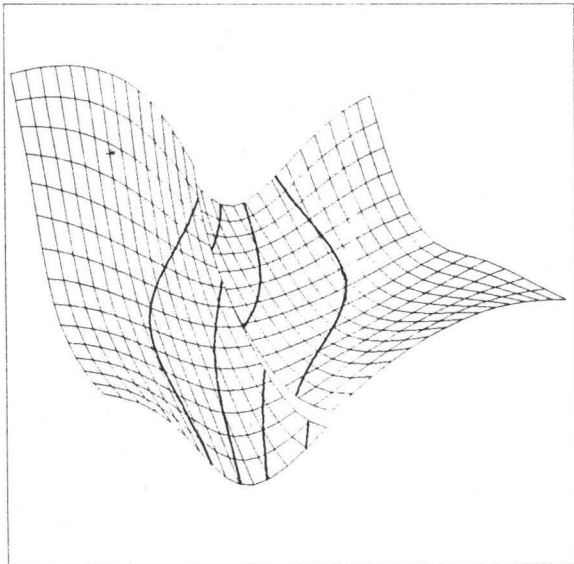


Fig. 13: Isophote surface with contours of $I(u, v) = \text{const.}$

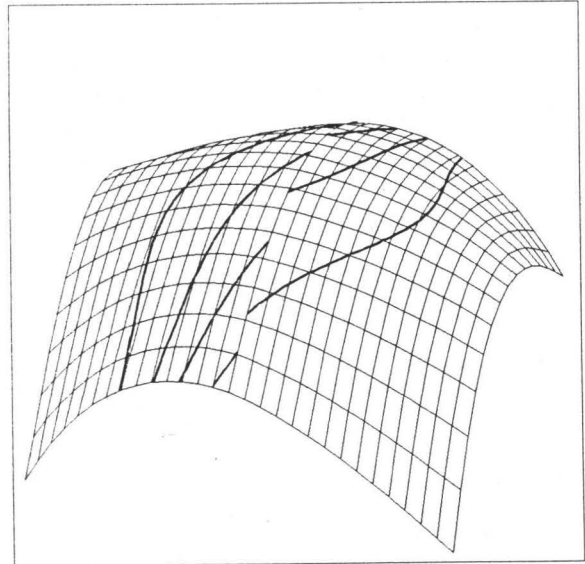


Fig. 14: C^0 -continuous surface with contours of $I(u, v) = \text{const.}$

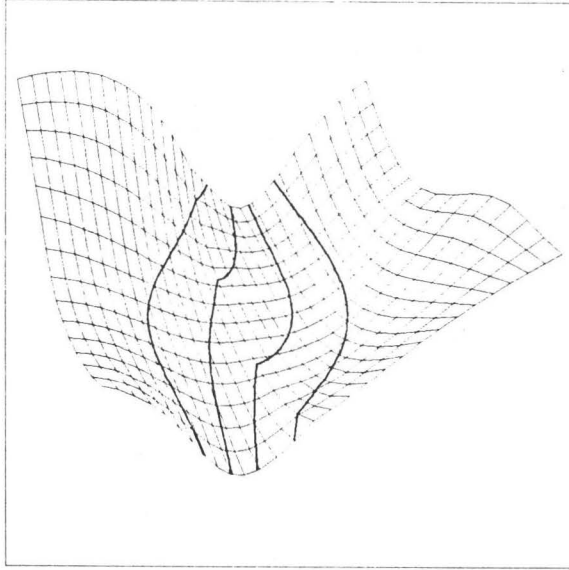


Fig. 15: Isophote surface with contours of $I(u, v) = \text{const.}$

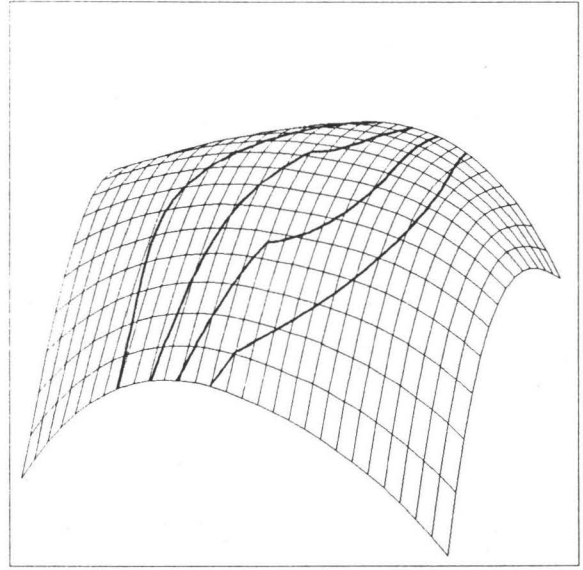


Fig. 16: G^1 -continuous surface with contours of $I(u, v) = \text{const.}$

4.4 Orthotomics

The *orthotomic* of an investigation surface $\mathbf{X}^{mn}(u, v)$ is a surface which is generated by reflecting a point P at all tangential planes of $\mathbf{X}^{mn}(u, v)$. A k -orthotomic is created, if the distance between P and the tangential plane is multiplied by the factor k . P must be neither on $\mathbf{X}^{mn}(u, v)$ nor on any tangential plane of $\mathbf{X}^{mn}(u, v)$ [4,14]. The irregularities of the surface $\mathbf{X}^{mn}(u, v)$ are projected onto singularities of the orthotomic surface $O(u, v)$. If $\mathbf{Y}(u, v)$ is the normal surface of $\mathbf{X}^{mn}(u, v)$ we get

$$O(u, v) = P + k \frac{\mathbf{Y}(u, v) \langle \mathbf{X}(u, v) - P, \mathbf{X}(u, v) \rangle}{\langle \mathbf{Y}(u, v), \mathbf{Y}(u, v) \rangle}. \quad (4.12)$$

The degree of $O(u, v)$ is $(5m-2, 5n-2)$ for non rational and $(9m-2, 9n-2)$ for rational investigation surfaces. Figure 17 shows the 2-orthotomic surface of the test surface from Section 4.1.

4.5 Polar Surfaces

The *polar surface* $\mathbf{P}(u, v)$ is the envelope of the planes, which is created by the mapping of all points of the investigation surface $\mathbf{X}^{mn}(u, v)$ by the polarity at the unit sphere in A [13].

$$\begin{aligned}
P(u, v) &= \frac{\mathbf{A}_u(u, v) \times \mathbf{A}_v(u, v)}{\det |\mathbf{A}_u(u, v), \mathbf{A}_v(u, v), \mathbf{A}(u, v)|} \\
&= \frac{\mathbf{A}_u(u, v) \times \mathbf{A}_v(u, v)}{\langle \mathbf{A}_u(u, v) \times \mathbf{A}_v(u, v), \mathbf{A}(u, v) \rangle}
\end{aligned}
\tag{4.13}$$

where $\mathbf{A}(u, v) = A - \mathbf{X}(u, v)$ with A not on $\mathbf{X}(u, v)$.

The degree of $P(u, v)$ is for non rational investigation surfaces $(3m - 1, 3n - 1)$ and for rational $(5m - 1, 5n - 1)$. Figure 18 displays the polar surface of the example from Section 4.1.

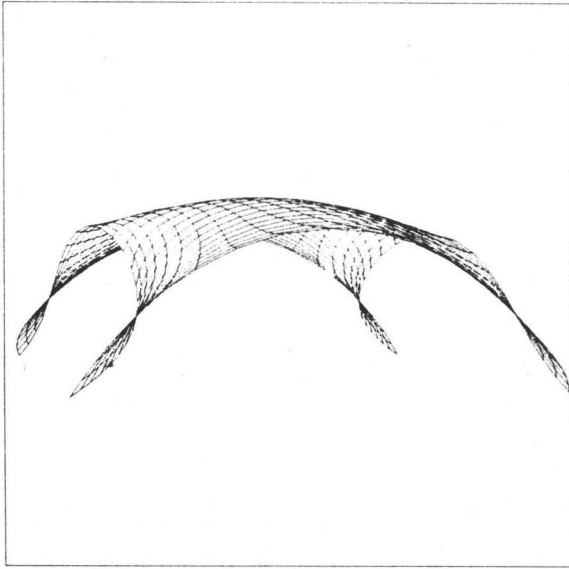


Fig. 17: 2-Orthotomic of the example surface

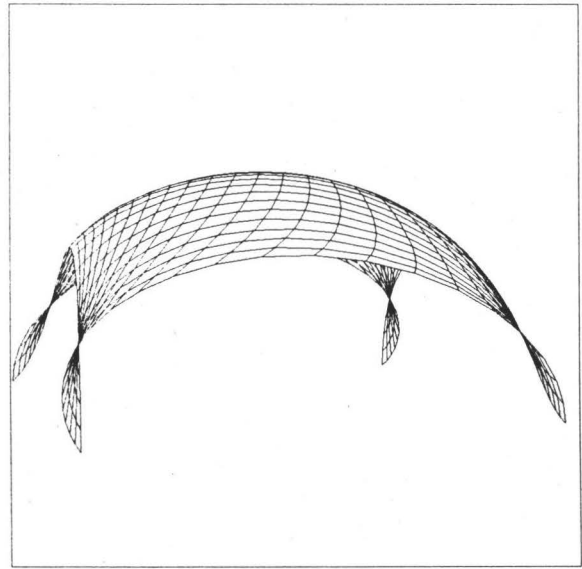


Fig. 18: Polar surface of the example surface

Visualizing $O(u, v)$ or $P(u, v)$ will point out the irregularities of $\mathbf{X}^{mn}(u, v)$. Finding of anomalies may be automated by using algorithms to detect self-intersections of Bézier surfaces.

5. Conclusions

We describe how to use arithmetic operations on Bézier surfaces for numerical stable calculations of accurate surface analysis methods. The resulting surfaces enable safe estimations from necessary conditions with respect to their Bézier net. This is, beside the easiness of the computation, the advantage of this method. On the other hand high surface degrees occur and make the subdivision algorithms more time consuming. With that we run into the usual trade off between accuracy and performance. A compromise may be the application of lower degree approximation surfaces (typically cubic) by degree

reduction [6] or least squared approximations [16]. By using the derivatives at least in the vertices, these approximations yield much better results as the approximation of pointwise generated values. Figure 19 and 20 show a bicubic C^0 -continuous approximation with 4 TPB of the Gaussian curvature surface of Figure 2 and Figure 4 respectively.

At this stage it should not be failed to mention, that in general a normalization in Euclidean space of a Bézier surface is not possible. Thus the square root has to be bypassed (see Section 4.3). Of course this is not always possible.

This method should be seen as a new tool for calculating with surfaces and should be used in applications which need a high level of accuracy and stability. It does not replace pointwise working algorithms. The best results are achieved by a good mixture of both depending on the application.

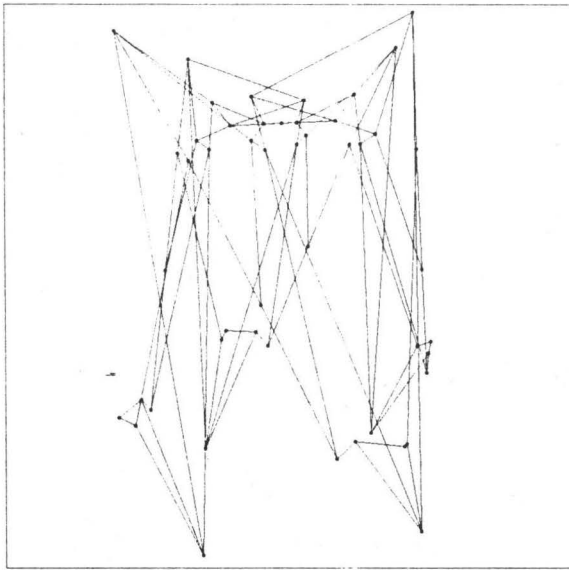


Fig. 19: Bézier net of 4 bicubic TPB approximation surfaces

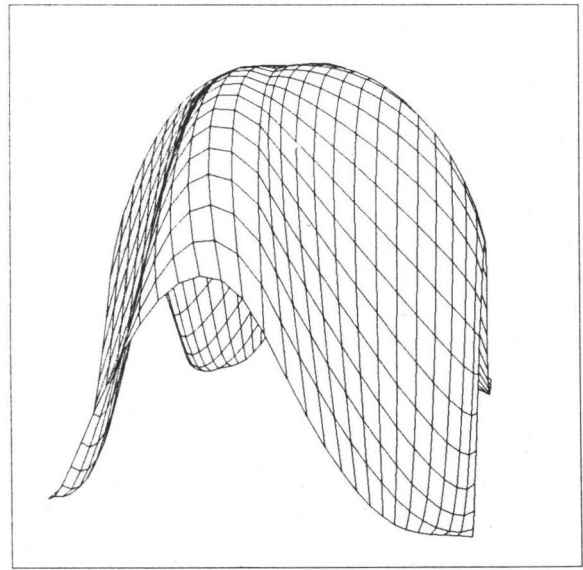


Fig. 20: TPB approximation of the Gaussian curvature surface

References

- [1] R. E. Barnhill, G. Farin, L. Fayard, H. Hagen: *Twists, curvatures and surface interrogation*, CAD, Vol.20, No.6, july/august, 1988, 341-346.
- [2] J. M. Beck, R. T. Farouki, J.K. Hinds: *Surface Analysis Methods*, IEEE CG&A, December 1986, 18-35.
- [3] W. Böhm, G. Farin, J. Kahmann: *A survey of curve and surface methods in CAGD*, CAGD 1 (1984) 1-60.
- [4] J. W. Bruce, P. J. Giblin, C. G. Gibson: *Caustics Through the Looking Glass*, The Math. Int., Vol. 6, No.1, 1984, 47-58.

- [5] G. Farin: *Triangular Bernstein-Bézier patches*, CAGD 3 (1986) 83–127.
- [6] G. Farin: *Algorithms for rational Bézier curves*, CAD, ?, 73–77.
- [7] G. Farin: *Curves and Surfaces for Computer Aided Geometric Design*, Academic Press 1991.
- [8] R. T. Farouki: *The approximation of non-degenerate offset surfaces*, CAGD 3 (1986) 15–43.
- [9] R. T. Farouki, V.T. Rajan: *On the numerical condition of Polynomials in Bernstein form*, CAGD 4 (1987) 191–216.
- [10] R. T. Farouki, V.T. Rajan: *Algorithms for polynomials in Bernstein form*, CAGD 5 (1988) 1–26.
- [11] H. Hagen, T. Schreiber, E. Gschwind: *Methods for Surface Interrogation*, Proc. Visualization '90, 187–193, (1990).
- [12] H. Hagen, S. Hahmann, T. Schreiber, Y. Nakajima, B. Wördenweber, P. Hollemann-Grundstedt: *Surface Interrogation Algorithms*, to be published in CG&A.
- [13] J. Hoschek: *Detecting regions with undesirable curvature*, CAGD 1 (1984) 183–192.
- [14] J. Hoschek: *Smoothing of curves and surfaces*, CAGD 2 (1985) 97–105.
- [15] J. Hoschek, D. Lasser: *Grundlagen der geometrischen Datenverarbeitung*, Teubner, 1989.
- [16] J. Hoschek, F. J. Schneider, P. Wassum: *Optimal approximate conversion of spline surfaces*, CAGD 6 (1989) 293–306.
- [17] E. Kaufmann, R. Klass: *Smoothing surfaces using reflection lines for families of splines*, CAD Vol.20, No.6, July/August 1988.
- [18] R. Klass: *Correction of Local Surface Irregularities using Reflection Lines*, CAD 12, 73–77, (1980).
- [19] E. Kreyszig: *Differentialgeometrie*, Leipzig, 1968.
- [20] M. Lipschutz: *Differentialgeometrie*, McGraw-Hill, 1980.
- [21] F. Munchmeyer: *Shape Interrogation: A Case Study*, Geometric Modeling, Algorithms and New Trends, Ed. G. Farin.
- [22] T. Poeschl: *Detecting surface irregularities using isophotes*, CAGD 1 (1984) 163–168.
- [23] H.-J. Schelske: *Lokale Glättung segmentierter Bézierkurven und Bézierflächen*, Dissertation, TH Darmstadt 1984.
- [24] L. L. Schumaker, W. Volk: *Efficient evaluation of multivariate polynomials*, CAGD 3 (1986) 149–154.
- [25] T. Schreiber: *Arithmetische Operationen auf Bézierflächen*, Interner Bericht 224/92, FB Informatik, Universität Kaiserslautern, Juni 1992.
- [26] M. A. Watkins, A. J. Worsey: *Degree reduction of Bézier curves*, CAD Vol.20, No.7, Sept. 1988, 398–405.